

Comparison of Models for Calculation of Diel Sediment-Water Heat Flux from Water Temperatures

Jordi Prats¹; Anaïs Ramos²; Joan Armengol³; and Josep Dolz, M.ASCE⁴

Abstract: We investigated sediment-water heat flux estimation in relation to applications (hydrodynamics simulation, evaporation studies, or global change effects assessment) in which sediment temperatures are not available because of technical complications (difficulties in installing sensors, for example) or because of methodology used (remote sensing, for example). We used field sediment temperature data measured every 10 min to 1 m depth at Doñana National Park marshland to obtain sediment thermal properties and to calculate diel sediment-water heat exchange through Beck's sequential function specification method. We compare four models for the simulation of sediment-water heat flux by using surface temperatures. Two models need initial estimated inside sediment temperatures; the other two do not. Influence of estimated initial temperature profiles depends on the temperature distribution assumption and is significant for three days or fewer at the daily timescale. A model that does not use initial sediment temperatures provides accurate estimations with low computation time. DOI: [10.1061/\(ASCE\)HY.1943-7900.0000434](https://doi.org/10.1061/(ASCE)HY.1943-7900.0000434). © 2011 American Society of Civil Engineers.

CE Database subject headings: Fourier series; Sediment; Water temperature; Hydraulic models.

Author keywords: Fourier series; Heat conduction; Sediment temperature; Sediment-water heat flux; Sequential function specification method.

Introduction

Interest in the physical modeling of lake and reservoir hydrodynamics has a long history, with a publishing record traceable to the 1960s (Raphael 1962; Delay and Seaders 1966; Edinger et al. 1968). Concern for environmental effects of cooling effluents and reservoirs was at the root of early modeling efforts (Raphael 1962; Delay and Seaders 1966; Edinger et al. 1974). These first modeling works generally neglected conduction through the water-sediment interface because of their small magnitude (Raphael 1962). They instead centered attention on heat exchange with the atmosphere (Edinger et al. 1968, 1974). Posterior research such as that by Brown (1969), Likens and Johnson (1969) and Jobson (1977) helped to assess the importance of sediment-water heat flux. Thanks to these and other works, we have learned that heat flux between water and sediment can have substantial effects on the heat balance in streams (Brown 1969; Jobson 1977; Sinokrot and Stefan 1993, 1994; Evans et al. 1998) and shallow lakes or reservoirs (Likens and Johnson 1969; Brutsaert 1982; Tsay et al. 1992) in annual (Tsay et al. 1992), daily (Jobson 1977; Sinokrot and Stefan 1993), and hourly timescales (Sinokrot and Stefan 1994).

In wetlands, observers have also noted that heat flux is prominent in daily timescales (Smith 2002). Sediment-water heat flux calculation is now included in many river and stream water-temperature models (Shen and Chiang 1984; Kim and Chapra 1997; Siviglia and Toro 2009) and lake hydrodynamics models (Tsay et al. 1992; Fang and Stefan 1996). Although the first 1D lake hydrodynamics models that included sediment-water heat flux did not consider it for all layers (Tsay et al. 1992), posterior developments calculated heat flux for all the layers of the water mass (Fang and Stefan 1996).

Sediment-water heat exchange can take place by different processes (conduction, convection, and advection), although it is usually calculated as a conduction process by using the heat conduction equation (Brutsaert 1982; Hondzo and Stefan 1994; Fang and Stefan 1998)

$$\frac{\partial T_b}{\partial t} = \alpha_b \frac{\partial^2 T_b}{\partial z^2} \quad (1)$$

in which $T_b(z, t)$ = riverbed temperature at depth z at time t , and α_b = sediment thermal diffusivity

$$\alpha_b = k_b / \rho_b C_b \quad (2)$$

in which k_b = sediment thermal conductivity, ρ_b = sediment density, C_b = volumetric heat capacity of the sediment. Eq. (1), with the necessary boundary conditions, can be solved numerically by finite differences (Sinokrot and Stefan 1993, 1994; Kim and Chapra 1997; Fang and Stefan 1998) or analytically. Analytical solutions used in water temperature models include the semi-infinite solid or homogeneous slab with an unsteady-state heat flux (Jobson 1977). It is far more common to consider a simplified sinusoidal surface flux (Brutsaert 1982; Tsay et al. 1992; Kim and Chapra 1997), although no analysis on the consequences of this simplification has been published.

Many solutions to the partial differential problem of Eq. (1) depend on boundary conditions, which often must be estimated. Given the difficulties in measuring sediment temperatures in water

¹Research Assistant, Civil Engineering School, Technical Univ. of Catalonia, C. Jordi Girona 1-3, Barcelona, 08034 Spain (corresponding author). E-mail: jordi.prats-rodriguez@upc.edu

²Researcher, Civil Engineering School, Technical Univ. of Catalonia, C. Jordi Girona 1-3, Barcelona, 08034 Spain. E-mail: anais.ramos@upc.edu

³Professor, Faculty of Biology, Univ. of Barcelona, Avda. Diagonal 645, Barcelona, 08028 Spain. E-mail: jarmengol@ub.edu

⁴Professor, Civil Engineering School, Technical Univ. of Catalonia, C. Jordi Girona 1-3, Barcelona, 08034 Spain. E-mail: j.dolz@upc.edu

Note. This manuscript was submitted on July 12, 2010; approved on April 1, 2011; published online on April 4, 2011. Discussion period open until March 1, 2012; separate discussions must be submitted for individual papers. This paper is part of the *Journal of Hydraulic Engineering*, Vol. 137, No. 10, October 1, 2011. ©ASCE, ISSN 0733-9429/2011/10-1135-1147/\$25.00.

bodies, sediment temperatures at different depths usually are lacking, and only the surface boundary condition, i.e., the temperature measured at the sediment surface or the water temperature, is available, because of the difficulty in installing temperature probes in great rivers and deep lakes or reservoirs. To overcome this problem, Jobson (1977) considered the initial condition a constant temperature profile. Fang and Stefan (1998) instead studied sediment temperature at 10 m, relating it to Secchi depth and lake geometry. Other options for confronting the problem consist of using theoretical solutions that do not require initial sediment temperatures, such as the sinusoidal surface heat flux. However, neither a comparison between different methods of estimating sediment-water heat flux nor the influence of different initial boundary conditions on heat flux estimations have been studied.

If enough sediment temperature information is available, one can calculate sediment-water heat exchange by integrating sediment temperature profiles and determining its rate of change (Tsay et al. 1992; Hondzo and Stefan 1994; Fang and Stefan 1998)

$$H_b = -\rho_b C_b \frac{\partial}{\partial t} \int_0^\infty T_b(z, t) dz \quad (3)$$

H_b is positive when sediment loses heat toward the water and negative when heat transfer from the water to the sediment. In spite of the simplicity of Eq. (3), sediment-water heat exchange calculation from measured sediment temperature is a severely ill-posed problem because of the sensibility of the solution of the inverse problem to measurement noise (Beck and Woodbury 1998). Diverse solutions to the 1D inverse heat conduction problem (IHCP) have been developed (Beck et al. 1996; Taler 1996; Ji et al. 1997; Beck and Woodbury 1998; Shenefelt et al. 2002). Notwithstanding the wide research in solving IHCPs, this methodology has scarcely been applied to water temperature modeling, with the exception of the work of Hondzo and Stefan (1994).

Apart from lake hydrodynamics modeling, calculating sediment-heat flux in water bodies can have hydrological applications, such as the calculation of evaporation by the heat balance method (Brutsaert 1982) or the estimation of groundwater flow (Silliman et al. 1995). Also, hyporheic temperatures influence life cycles and metabolic rates of benthic communities and fish egg development (Shepherd et al. 1986; Evans and Petts 1997; Malcolm et al. 2002; Smith 2002). As a result, given the concern for global change consequences, which include reduced precipitation, higher temperatures, and higher evapotranspiration in the Iberian Peninsula (Moreno 2005), sediment-water heat flux simulation can interest those in water resources management and in estimating climate change ecological effects. Of special interest would be developing accurate ways to estimate sediment-water heat flux from water temperatures in relation to remote sensing and global change applications, in which sediment temperatures are usually unknown (Holmes et al. 2008).

In this paper, sediment temperature is measured every 10 min at different depths between the surface and 1 m deep at Doñana National Park marshland. We use Beck's sequential function specification method (SFSM) to calculate sediment-water heat flux from sediment temperatures, to overcome the important measurement noise from water temperature variation caused by the short time step. We estimate sediment-water heat exchange from surface temperature by using different models on the daily timescale: (1) the general theoretical solution of the heat conduction equation and estimated-depth varying temperature profile, (2) the same general solution and constant estimated initial temperature profile, (3) the solution of the heat conduction equation, assuming the surface sediment temperature to be a time-dependent harmonic function, and (4) the solution of the heat conduction equation for a sinusoidal

surface temperature. The last two cases do not require an initial profile. We compare here the results obtained with the different models.

Study Area and Instrumentation

We undertook this study in the marshland of Doñana National Park in southwest Spain, in the Guadalquivir River estuary. The park measures 54,252 ha, of which 27,000 ha are marshland. This is one of the most important wetlands in the Iberian Peninsula. To inform management decisions, we conducted some research in course to apply a numerical hydrodynamic model to Doñana wetland (Dolz et al. 2005; Bladé and Gómez 2006) using remote sensing (Marti-Cardona et al. 2010) and hydrometeorological data. Since autumn 2004, our research group has used measuring stations within Doñana National Park to collect meteorological, water temperature, and water level data (Fig. 1). At some of these stations, we also installed Campbell Pt100 thermistors (precision 0.1°C) to measure sediment temperature. We installed double probes at different depths (0.01, 0.25, 0.5, 0.75, 1.00 m) in the sediment. We measured temperature every 1 min and saved the mean every 10 min in Campbell dataloggers. The data were periodically downloaded by modem.

In this paper, data from two stations are used: Lucio del Lobo (Universal Transverse Mercator [UTM] coordinates 29 N $x = 736346$ $y = 4106237$) from December 5, 2004 to April 23, 2005, and Lucio de Vetalengua (UTM 29N $x = 733189$ $y = 4089572$) from October 18, 2006 to July 16, 2007. In both cases, the marshes were flooded throughout the study period (Fig. 2). The marshes usually begin to flood between October and November, depending on precipitation and inflows (García and Marín 2005). From February to March, the marshes attain equilibrium between inflows and evapotranspiration. The area subsequently dries when evapotranspiration increases and precipitation diminishes. During the summer, the marshes are dry.

Some blanks exist in the Lucio del Lobo data series because of instrumentation breakdowns. The sensors installed at 0.5 m malfunctioned shortly after installation and could not be replaced during the study period. Fig. 3 shows the air temperature measured at Lucio del Lobo and Lucio de Vetalengua stations.

Methods

We calculated sediment-water heat exchange from the measured sediment temperature data, applying Beck's SFSM (Beck et al. 1985, 1996; Beck and Woodbury 1998) to solve the IHCP. We then used four different mathematical models based on theoretical solutions to the heat conduction equation, in addition to different initial and boundary conditions, to estimate the same heat flux. We implemented the models in Matlab 7.0 (R14) (MathWorks, Natick, MA) using predetermined sediment thermal properties and compared results obtained with the different models.

Heat Exchange Calculation

Beck's SFSM is a simple, computationally efficient sequential method that uses sediment temperature sensitivities and future sediment temperature measurements to calculate heat flux (Beck et al. 1985, 1996; Beck and Woodbury 1998). In brief, the method minimizes the sum of square errors function for the R future measurements to obtain the expression of heat flux at time t_M

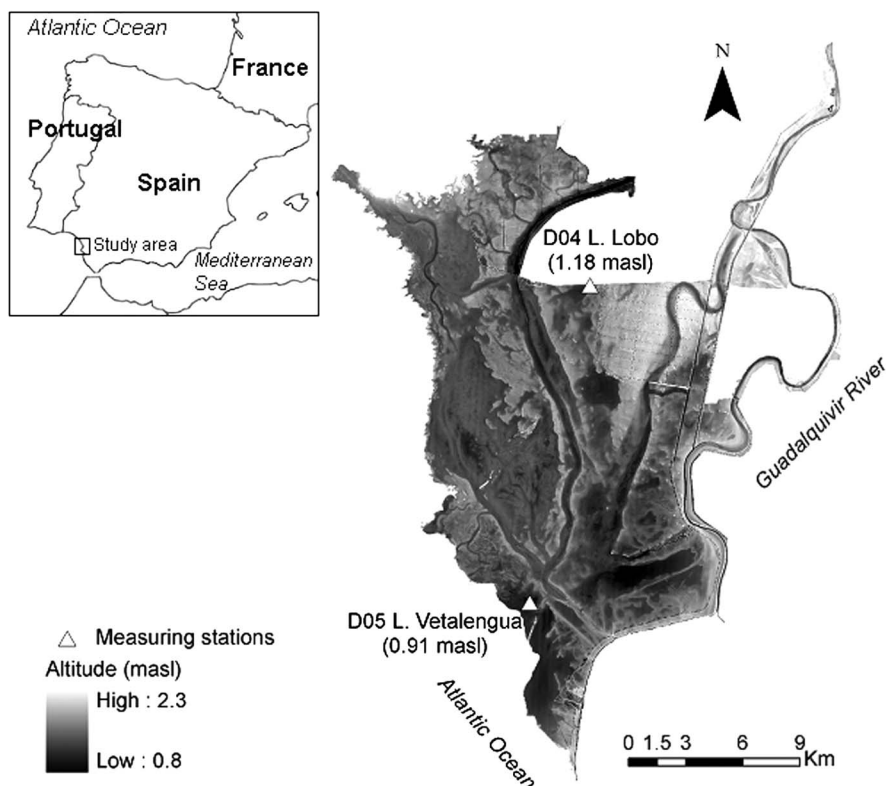


Fig. 1. Doñana National Park marshland and measuring stations; elevation color scale and site elevation at each station

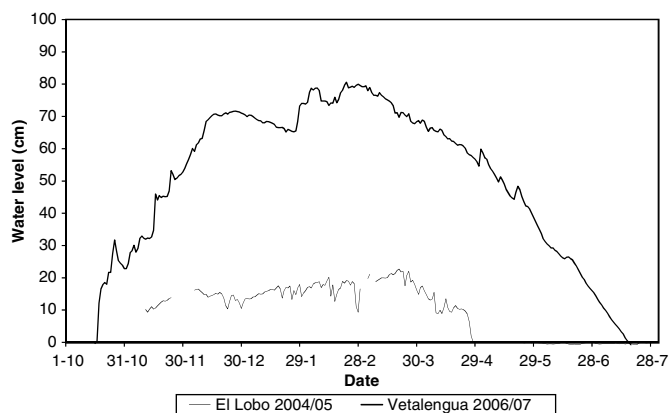


Fig. 2. Mean daily water level at Lucio del Lobo (hydrologic year 2004–2005) and Lucio de Vetalengua (hydrologic year 2006–2007) stations

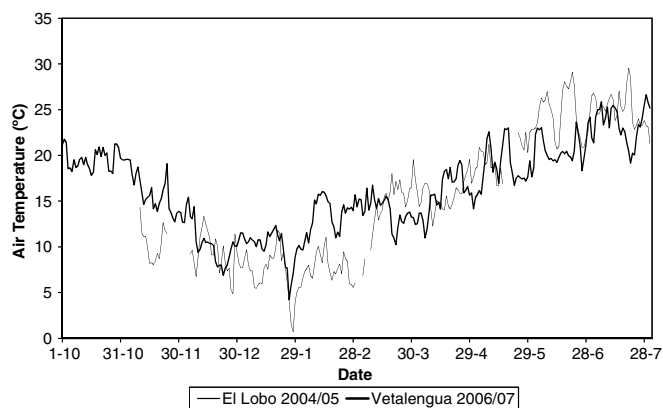


Fig. 3. Mean daily air temperature at Lucio del Lobo (hydrologic year 2004–2005) and Lucio de Vetalengua (hydrologic year 2006–2007) stations from October 1–July 31

$$H_b(t_M) = \frac{\sum_{i=1}^R \left(\hat{T}_{M+i-1} - \sum_{k=1}^{M-1} H_b(t_k) \Delta \varphi_{M-k+i-1} - T_0 \right) \varphi_i}{\sum_{i=1}^R \varphi_i^2} \quad (4)$$

in which heat flux $H_b(t_M)$ is assumed to be constant from time t_{M-1} to t_{M+R-1} , $\hat{T}_i = \hat{T}(z, t_i)$ = estimated temperature at depth z , and time t_i , $T_0 = T(z, 0)$ = initial measured temperature at depth z ; $\varphi_i = \varphi(z, t_i)$ are sensitivity coefficients of sediment temperature to heat flux at depth z and time t_i , and

$$\Delta \varphi_i = \varphi_{i+1} - \varphi_i \quad (5)$$

We used $R = 3$ future measurements to avoid errors derived from using future times (Beck et al. 1985). Beck's method allows the

calculation of heat flux by using sediment temperatures at any single depth inside the sediment, but also from two or more sediment temperature signals measured at different depths. We applied the method only to the surface sensor to obtain the sediment-water heat flux, because when applied to deeper sensors the method became unstable. Beck's method stability depends on the temporal discretization and the number of future measurements used (R). One may obtain stability by increasing R or by decreasing the discretization (Liu 1996). Because we took measurements every 10 min, we could not reduce the discretization. Then, daily heat waves needed several hours to attain 0.25 m depth. Consequently, for such a small discretization, we would have needed to increase R considerably, with a significant associated error increment.

Heat Exchange Simulation

The theoretical solutions from which we derived the models are the general solution of the heat conduction equation for a homogeneous semi-infinite solid, and the solution for the same type of solid when surface temperature is a harmonic function of time or can be expressed as a time-dependent Fourier series. Carslaw and Jaeger (1959) included both solutions. We smoothed sediment temperatures given as input for the models with a 1 h moving average to filter out part of the measurement noise.

Models M1 and M2

We obtained Models M1 and M2 from the general solution of the heat conduction equation for a semi-infinite solid (Carslaw and Jaeger 1959) using a different initial condition for each model. Models M1 and M2 differ in their initial condition $f(z)$. In model M1, the initial condition is the expected temperature profile if the surface temperature has a sinusoidal behavior along the year

$$f_1(z) = T_{b,y} + C_y e^{-\eta_y z} \cos(\omega_y t - \eta_y z + e_y) \quad (6)$$

in which $\omega_y = 2\pi/1$ year, $\eta_y = \sqrt{\omega_y/2\alpha_b}$, and making $t = 0$. One can estimate the mean local groundwater temperature, $T_{b,y}$, from mean annual air temperature (Todd 1980; Fang and Stefan 1998) and we assigned a value of 19.09°C to it for both stations. We estimated the annual surface temperature amplitude C_y (9.78°C at Lucio del Lobo and 6.86°C at Lucio de Vetalegua) and phase e_y (2.58 at Lucio del Lobo and 3.07 at Lucio de Vetalegua) by least squares using the experimental data for $z = 0$. The estimated initial profile was a rather rough guess at Lucio del Lobo, with a correlation coefficient of 0.37 and mean error of 1.31°C, but more accurate for Lucio de Vetalegua station, with a correlation coefficient of 0.89 and mean error of -0.48°C. In model M2, we assumed initial temperature to be constant in the entire profile and equal to surface initial temperature

$$f_2(z) = T_b(0, 0) \quad (7)$$

When no sediment temperature data are available, this is often the only initial condition hypothesis that one can take into account (e.g., Jobson 1977).

Assuming the initial and boundary conditions are

$$T_b(z, 0) = f(z) \quad T_b(0, t) = g(t) \quad (8)$$

in which $f(z)$ = sediment initial temperature and $g(t)$ = sediment surface temperature (which is equal to the water temperature), the general solution of the heat conduction equation for a homogeneous solid is

$$T_b(z, t) = 2/\sqrt{\pi} \int_0^\infty g(t - z^2/4\alpha_b\mu^2) e^{-\mu^2} d\mu + 1/2\sqrt{\pi\alpha_b t} \int_0^\infty f(\lambda) \left[e^{-\frac{(z-\lambda)^2}{4\alpha_b t}} - e^{-\frac{(z+\lambda)^2}{4\alpha_b t}} \right] d\lambda \quad (9)$$

where the parameters μ and λ are integration variables. This method allows sediment temperature to be calculated according to depth and time.

Once we know sediment temperature, we obtain sediment-water heat exchange through numerical integration of Eq. (3) down to a given depth L . The integration depth depends on the duration of the heat flux. For diurnal water temperature variation, the sensitive bed thickness is only 0.25–0.30 m (Jobson 1977; Hondzo and Stefan 1994), and for a heat flux of 1 wk, the sensitive thickness is 0.80 m (Hondzo and Stefan 1994). For the seasonal timescale, heat storage does not penetrate significantly below 6 m (Hondzo et al. 1991), and a depth of 10 m has also been used (Fang and Stefan 1996, 1998). In this paper, we made calculations for integration depths of 6 and 10 m, and we observed no significant difference. We present results for $L = 10$ m only. Assuming the initial boundary condition implies the possibility of a significant difference in the actual initial temperature. Consequently, at the beginning of the study period the estimated heat flux is not reliable, and as the simulation time advances, the estimated values converge to the real values. If estimated initial temperatures differ importantly from actual initial temperatures, the time of convergence can be very long (Fang and Stefan 1998). In our case, calculations showed that after three days the error of the heat flux estimations stabilized (Fig. 4). Therefore, when H_b is calculated using model M1 or M2 for a given time period, the calculations were initiated three days

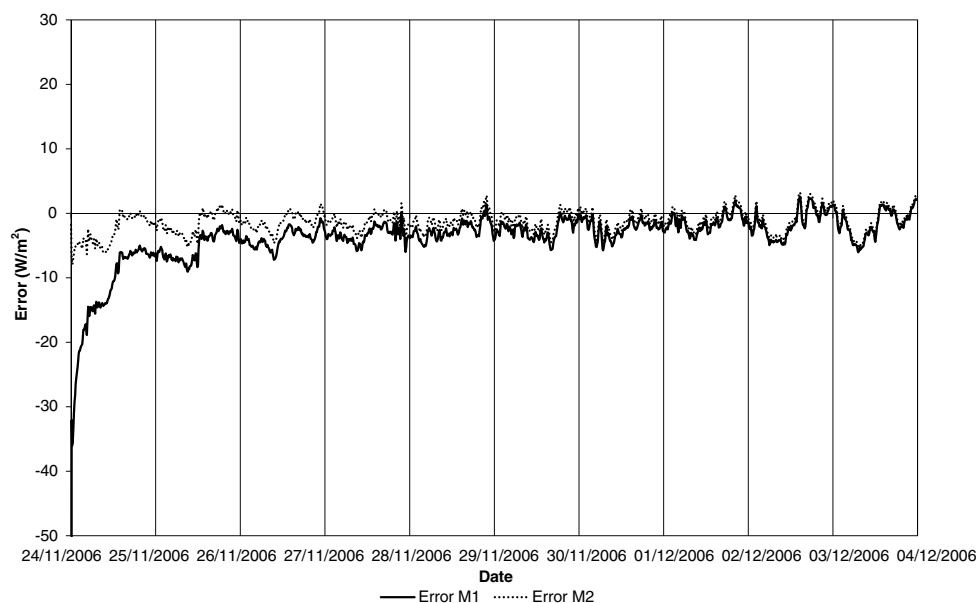


Fig. 4. Estimation error of Models M1 and M2 in a 10-day period (November 24, 2006–December 3, 2006) at Lucio de Vetalegua station

beforehand. Afterward, we used only the values corresponding to the period of interest.

Model M3

Model M3 uses the solution of the heat conduction equation for a semi-infinite solid when the surface temperature is a harmonic function of time (Carslaw and Jaeger 1959). In particular, model M3 uses the simplest case, which consists of assuming that the surface temperature has a daily sinusoidal behavior such as

$$T_b(0, t) = T_{b,d} + C_d \cos(\omega_d t + e_d) \quad (10)$$

in which C_d , ω_d , and e_d = amplitude, angular frequency, and phase of the sinusoidal surface temperature, respectively, and $T_{b,d}$ is the mean daily temperature at the surface. We can then express the sediment temperature in the steady state as

$$T_b(z, t) = T_{b,d} + C_d e^{-\eta_d z} \cos(\omega_d t - \eta_d z + e_d) \quad (11)$$

in which $\omega_d = 2\pi/1\text{day}$, $\eta_d = \sqrt{\omega_d/2\alpha_b}$. Thus, from Eqs. (3) and (11), the sediment-water heat exchange is

$$H_b = -\rho_b C_b \frac{\partial}{\partial t} \int_0^\infty T_b(z, t) dz = C_d C_b \sqrt{\omega_d \alpha_b} \sin(\omega_d t + e_d - \pi/4) \quad (12)$$

Furthermore, making $t = 0$ in Eq. (11) obtains an initial condition of the f_1 kind [Eq. (6)].

Moreover, deriving Eq. (11) for $z = 0$, we obtain the surface temperature variation as

$$\left. \frac{\partial T_b}{\partial t} \right|_{z=0} = -C_d \omega_d \sin(\omega_d t + e_d) \quad (13)$$

Considering that in our case the period = 1 day, a $n/4$ rad phase difference = 3 h. Thus, from Eqs. (12) and (13), we can write the relation between H_b and the temperature variation at the surface as

$$H_b = -\rho_b C_b \sqrt{\frac{\alpha_b}{\omega_d}} \left. \frac{\partial T_b(z, t - \delta)}{\partial t} \right|_{z=0} \quad (14)$$

with $\delta = 3$ hours. Although one could estimate T_b in Eq. (14) by fitting Eq. (11) by least squares, in this paper we assumed measured surface sediment temperature to be approximately sinusoidal, and we substituted directly in Eq. (14). One of the most notable characteristics of this method is that an initial condition is not necessary.

Model M4

Model M4 is based on the same theoretical solution as model M3, but it takes into account the more complex case of expressing the surface temperature as a Fourier series

$$T_b(0, t) = T_{b,d} + \sum_{n=1}^N C_n \cos(n\omega_f t + e_n) \quad (15)$$

in which N = number of harmonics and

$$\omega_f = 2\pi/P \quad (16)$$

= fundamental frequency, with P = length of time of the data segment. C_n and e_n = amplitude and phase of the n th harmonic, respectively. We made $N = 24$ times the number of days of the period of interest, so that the maximum frequency we used was 1.0 h^{-1} . We calculated H_b as

$$H_b(t) = \rho_b C_b \sum_{n=1}^N C_n \sqrt{n\omega_f \alpha_b} \sin(n\omega_f t + e_n - \pi/4) \quad (17)$$

C_n and e_n can be expressed as

$$C_n = \sqrt{A_n^2 + B_n^2} \quad (18)$$

$$e_n = \tan^{-1}(-B_n/A_n) \quad (19)$$

with

$$A_n = \frac{2}{M} \sum_{i=1}^M T_b(0, t_i) \cos \frac{2\pi n i}{M} \quad (20)$$

$$B_n = \frac{2}{M} \sum_{i=1}^M T_b(0, t_i) \sin \frac{2\pi n i}{M} \quad (21)$$

in which M = total number of measurements in the period P .

We calculated Fourier coefficients for each week in the study period. However, an overshoot of the Fourier series occurring at discontinuity points, known as Gibbs phenomenon (Braun 2008), often appeared at both extremes of the series of interest. To overcome this problem, we added the previous and subsequent days to the series of interest to fit the Fourier series. Consequently, because the period of interest was 1 week, the data series used for the calculations was 9 days. At the end of the process, we took only the data corresponding to the period of interest and discarded the extremes. Mean values of the Fourier parameters C_n and e_n appear in Fig. 5. Agreement between measured sediment surface temperatures and temperatures estimated by Fourier series was very high, with mean square errors of the order of $10^{-3} \text{ }^\circ\text{C}^2$ and correlation coefficients of 0.999.

Thermal Properties

In aquatic ecosystems, thermal diffusivity α_b can take values between 0.12 and $1.27 \times 10^{-6} \text{ m}^2\text{s}^{-1}$ (Fang and Stefan 1998). In this study, we determined α_b from the solution to the heat conduction equation for a sinusoidal surface temperature. Temperature fluctuations travel at a rate of $\sqrt{2\alpha_b\omega}$ (Carslaw and Jaeger 1959). We fitted Eq. (11) for the different depths z by least squares to the measured surface temperature using all measurements for each day of the study period and for both stations. We selected the days with a better fit ($r > 0.98$). For these days, we calculated the time required for the maximum daily temperature to reach 0.25 m depth. We used this value to calculate α_b for each of the selected days. At Lucio del Lobo, 16 of 106 cases fulfilled the chosen conditions. The thermal diffusivity at this station showed a value of $3.28 \times 10^{-7} \text{ m}^2\text{s}^{-1}$ (95% confidence interval of $2.92 - 3.63 \times 10^{-7} \text{ m}^2\text{s}^{-1}$). At Lucio de Vetalengua, we met conditions on 38 of 270 cases. The estimated value was slightly lower: $2.07 \times 10^{-7} \text{ m}^2\text{s}^{-1}$ (95% confidence interval of $2.02 - 2.12 \times 10^{-7} \text{ m}^2\text{s}^{-1}$).

The sediment-heat capacity, $\rho_b C_b$, of lakes and rivers lies in the range $1.4 - 3.8 \times 10^6 \text{ J }^\circ\text{C}^{-1} \text{ m}^{-3}$, depending on their composition (Hondzo and Stefan 1994; Fang and Stefan 1998). Moreover, several authors (Likens and Johnson 1969; Jobson 1977; Tsay et al. 1992; Silliman et al. 1995; Kim and Chapra 1997; Fang and Stefan 1998) have used values between $2.0 - 4.2 \times 10^6 \text{ J }^\circ\text{C}^{-1} \text{ m}^{-3}$ in their models to estimate sediment-water heat exchange, although the most frequently used values are approximately $2.0 - 2.5 \times 10^6 \text{ J }^\circ\text{C}^{-1} \text{ m}^{-3}$.

One can estimate sediment-heat capacity using the volume fractions of the different sediment components (Brutsaert 1982; Hondzo and Stefan 1994)

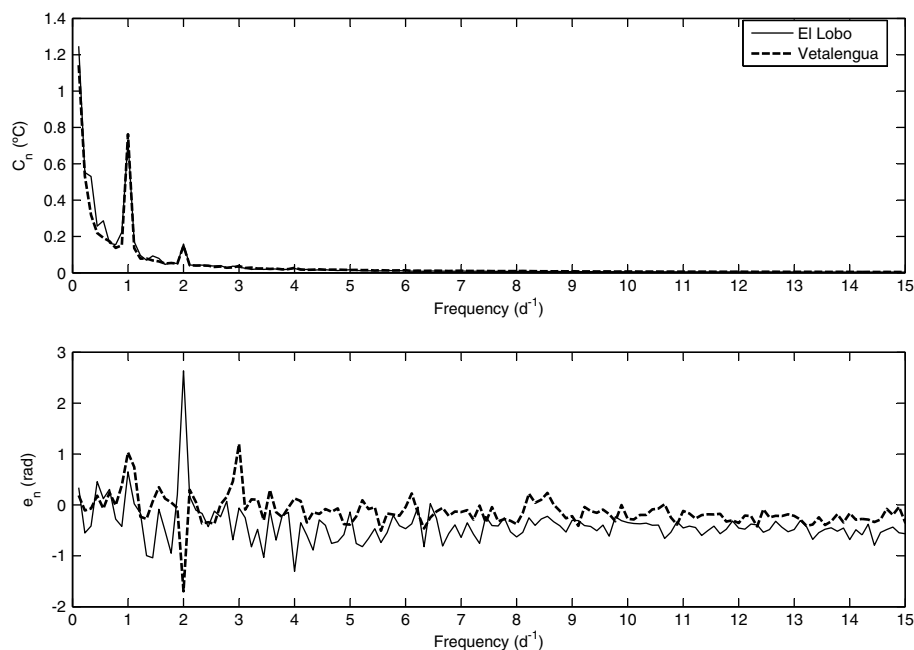


Fig. 5. Fourier coefficients for Lucio del Lobo and Lucio de Vetallengua stations (Doñana National Park); mean of all weeks studied

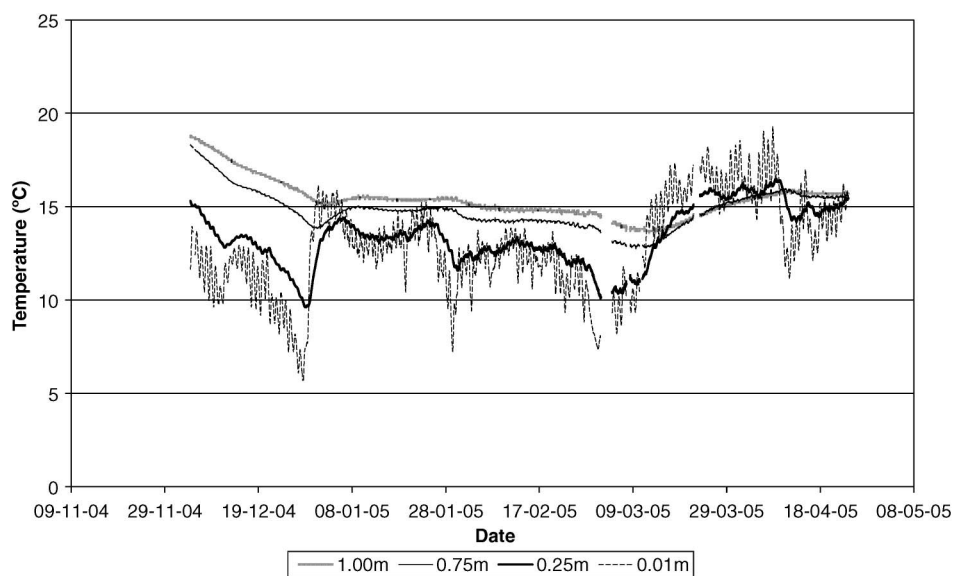


Fig. 6. Sediment temperature at different depths, Lucio del Lobo (Doñana National Park), December 5, 2004–April 23, 2005

$$\rho_b C_b = \rho_m \theta_m C_m + \rho_c \theta_c C_c + \rho_w \theta_w C_w + \rho_a \theta_a C_a \quad (22)$$

in which ρ_* = density, θ_* = volume fraction, and C_* = volumetric heat capacity of the sediment (b) and of its components: mineral (m), organic matter (c), water (w), air (a). In aquatic ecosystems, the sediment is usually saturated. Then Eq. (22) can be simplified, giving

$$\rho_b C_b = \rho_m \theta_m C_m + \rho_c \theta_c C_c + \rho_w \theta_w C_w \quad (23)$$

Doñana marshland sediment mainly contains fine silt, clay, and sand (Ruiz et al. 2004; Reina et al. 2006). The organic matter content in the sediment is about 5% of dry weight in nonvegetated zones and about 6–8% in areas covered by macrophytes (Reina et al. 2006). Water content in marsh sediments was observed to

be between 50 and 200% of the dry weight, depending on draining conditions and the consolidation degree of the sediment (Crooks et al. 2002). The heat capacities of the main components of Doñana National Park marshland are $4.166 \times 10^6 \text{ J}^\circ\text{C}^{-1}\text{m}^{-3}$ for water, $1.212 \times 10^6 \text{ J}^\circ\text{C}^{-1}\text{m}^{-3}$ for sand, $1.285 \times 10^6 \text{ J}^\circ\text{C}^{-1}\text{m}^{-3}$ for clay, and $2.504 \times 10^6 \text{ J}^\circ\text{C}^{-1}\text{m}^{-3}$ for organic matter (Brutsaert 1982; Incropera and DeWitt 1996). Taking into account the range in variation of water content in marsh soils found by Crooks et al. (2002), the organic matter content observed by Reina et al. (2006), and the fact that the heat capacities of sand and clay are very similar, we can deduce from Eq. (23) that sediment-heat capacity in Doñana National Park should be between $2.2 - 3.2 \times 10^6 \text{ J}^\circ\text{C}^{-1}\text{m}^{-3}$. In this paper, we use the mean value of this range, which is $2.7 \times 10^6 \text{ J}^\circ\text{C}^{-1}\text{m}^{-3}$.

Goodness of Fit

We assessed the goodness of fit of the models according to the mean square error (MSE) and the correlation coefficient (r) of the mean daily heat flux estimations in relation to the heat flux calculated by applying Beck's SFSM. We interpolated linearly the temperature between the measurement points.

Results

Measured Temperature

The soil temperature at the surface is equal to the water temperature. The daily variations of temperature weaken quickly with depth, whereas the variations at longer periods are visible even to a depth of 1 m, although they have a lower amplitude and a

certain delay (Fig. 6). The sediment temperature at the surface at Lucio del Lobo station varied between 6 and 19°C in the study period, whereas at 1 m depth, it varied between 13 and 19°C. The mean daily range of temperature at the surface was about 2°C (Fig. 7), although on December 29, 2004, the daily range reached 5°C because of a significant increase in air temperature. At 0.25 m, the mean range was 0.4°C, whereas at 0.75 and 1.0 m the range only reached 0.1–0.2°C, which was little more than the precision of the temperature probe.

The measurements we took at Lucio de Vetallengua station from October 18, 2006 to July 16, 2007 showed similar characteristics (Fig. 8). The sediment temperature at the surface decreased beginning in October. In January 2007, it began to increase and remained at values between 6°C at the end of January and 31°C in July. At greater depths, the temperature followed the same trend, but the thermal amplitude was weaker and had a delay that increased

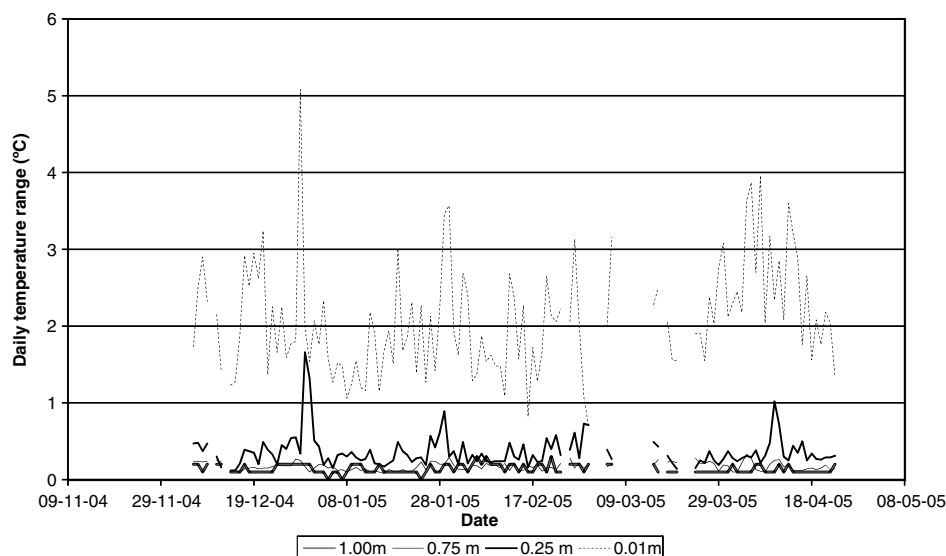


Fig. 7. Daily range of sediment temperature at different depths, Lucio del Lobo (Doñana National Park), December 5, 2004–April 23, 2005; gaps exist in the temperature data series

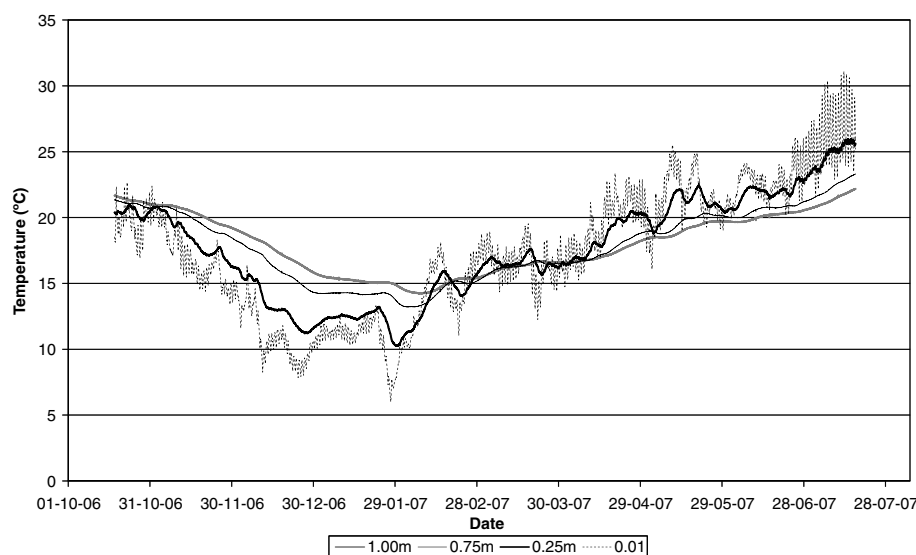


Fig. 8. Sediment temperature at different depths, Lucio de Vetallengua (Doñana National Park), October 18, 2006–July 16, 2007

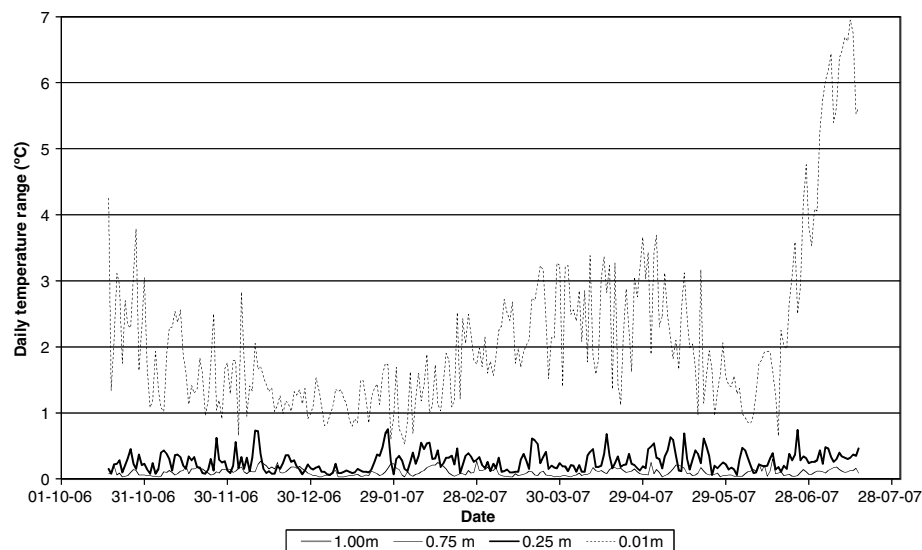


Fig. 9. Daily range of sediment temperature at different depths, Lucio de Vetalegua (Doñana National Park), October 18, 2006–July 16, 2007

with depth. At 1 m, the temperature remained between approximately 14–24°C. The range of variation of the surface temperature fluctuated throughout the study period (Fig. 9). In October 2006, it was approximately 2.5°C, and it decreased to approximately 1°C at the end of the year. In April 2007 it rose to values of approximately 2.5°C. From April until mid-June 2007, the mean daily range decreased. Finally, near the end of the study period, the range of daily temperature variation increased notably because of the low water level (Fig. 2) and high incoming solar radiation. At 0.25m, the mean daily range was 0.3°C; at greater depths it was approximately 0.1°C.

Sediment-Water Heat Exchange

Fig. 10 shows the mean daily value of H_b and the daily maxima and minima from December 5, 2004, to April 23, 2005, at Lucio del Lobo. Fig. 11 shows the same variables at Lucio de Vetalegua from October 18, 2006, to July 16, 2007. The mean daily sediment-water heat exchange generally was low, and in absolute values,

it rarely exceeded 10 W/m². The mean daily heat exchange was more than 10 W/m² for 6% of the study period at Lucio del Lobo and only 0.4% of the study period at Lucio de Vetalegua. At Lucio del Lobo, at the end of December 2004, we observed heat loss from sediment to water with a mean daily value of as much as −17 W/m². The cause was a sharp increase in water temperature of 7°C within three days (Fig. 4). H_b showed a daily cycle varying between approximately −30 and 30 W/m² during the day. We observed the maximum H_b values in the morning (0800–1000 h, solar time) and the minimum values in the afternoon (1600–1800 h, solar time). At Lucio del Lobo, the minimum values of H_b occasionally attained −50 W/m², and the maximum values attained 35 W/m². At Lucio de Vetalegua, however, heat flux variability depended on the time of year. In December and January, H_b varied between −10 and 10 W/m². At the end of June, however, the thermal range increased, attaining a daily maximum of 32 W/m² and a minimum of −55 W/m² because of a reduction in the water level.

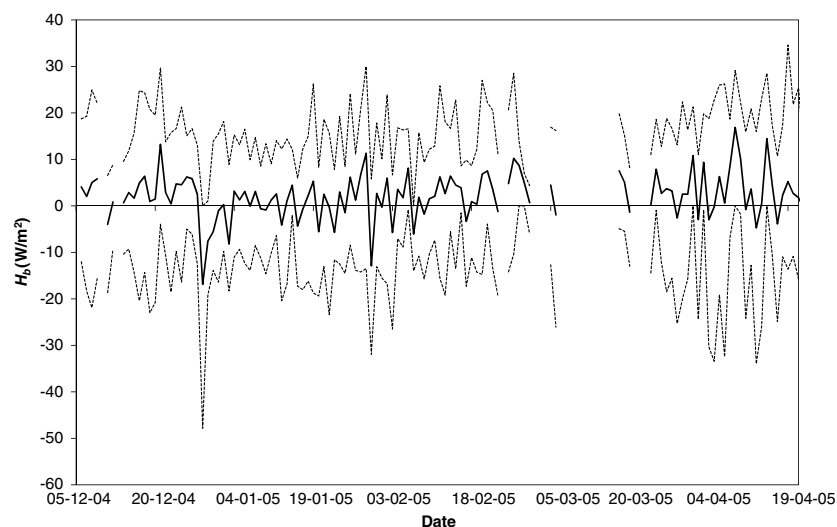


Fig. 10. Mean daily sediment-water heat exchange (solid line) and daily maxima and minima (broken lines), Lucio del Lobo (Doñana National Park), December 5, 2004–April 23, 2005

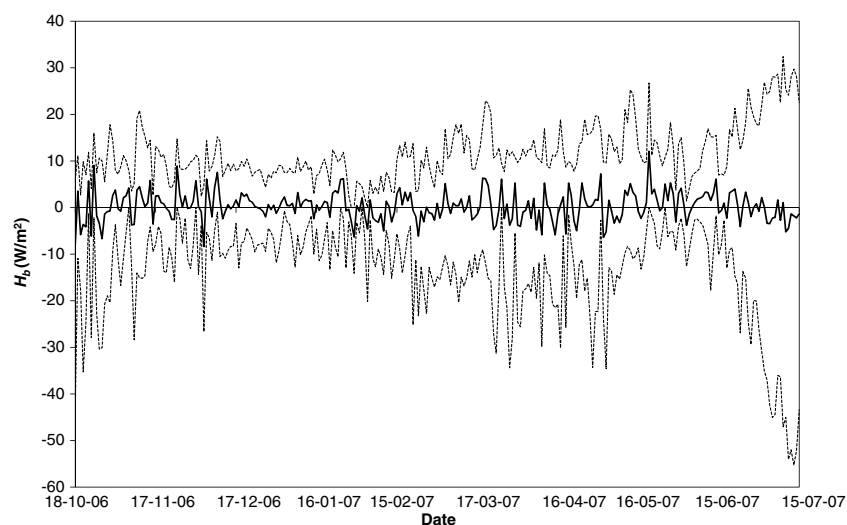


Fig. 11. Mean daily sediment-water heat exchange (solid line) and daily maxima and minima (broken lines), Lucio de Vetallengua (Doñana National Park), October 18, 2006–July 16, 2007

Table 1. Mean Square Error (MSE) and Correlation Coefficient of Mean Daily H_b Estimated Using Different Models in Relation to Measured Heat Exchange

Models	Lucio del Lobo		Lucio de Vetallengua	
	MSE ($^{\circ}C^2$)	r	MSE ($^{\circ}C^2$)	r
M1	17.90	0.96	9.03	0.95
M2	9.08	0.97	9.88	0.94
M3	57.39	0.80	28.87	0.81
M4	9.57	0.97	5.78	0.97

Model Behavior

Calculation time of the heat exchange every 10 min during a week using a program compiled in MATLAB on a Pentium 4, 3.4 GHz computer was negligible for model M3, was 0.4 s for model M4, and was approximately 400 s for models M1 and M2. The results of model behavior appear in Table 1. According to the MSE results, M2 and M4 were the most accurate models at Lucio del Lobo, and M1 and M4 were the most accurate at Lucio de Vetallengua. Model M3 was the least accurate of all cases. As for the correlation coefficient, Model M4 produced the best results at both stations;

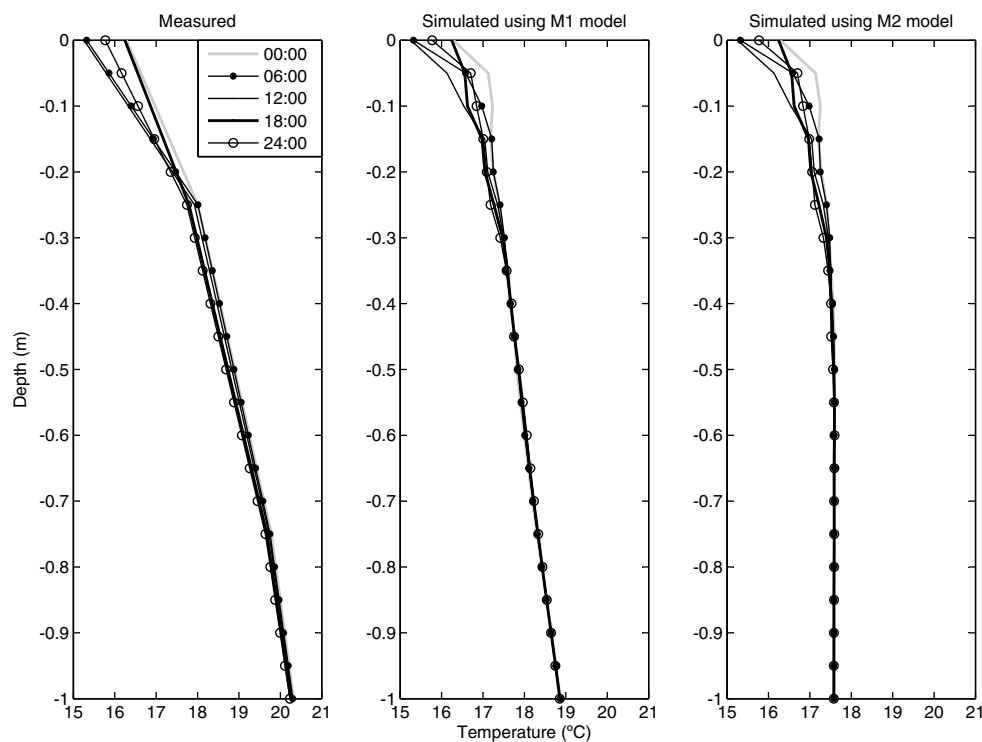


Fig. 12. Sediment temperature profiles measured and simulated with Models M1 and M2, Lucio de Vetallengua (Doñana National Park), November 29, 2006

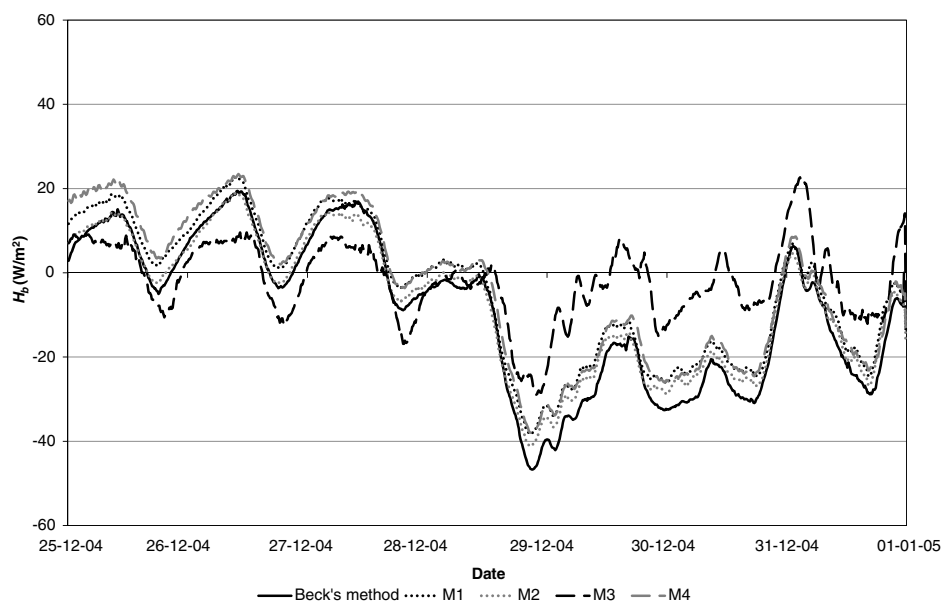


Fig. 13. Sediment-water heat exchange, calculated with Beck's method and estimated with Models M1–M4 from December 25, 2004–January 1, 2005

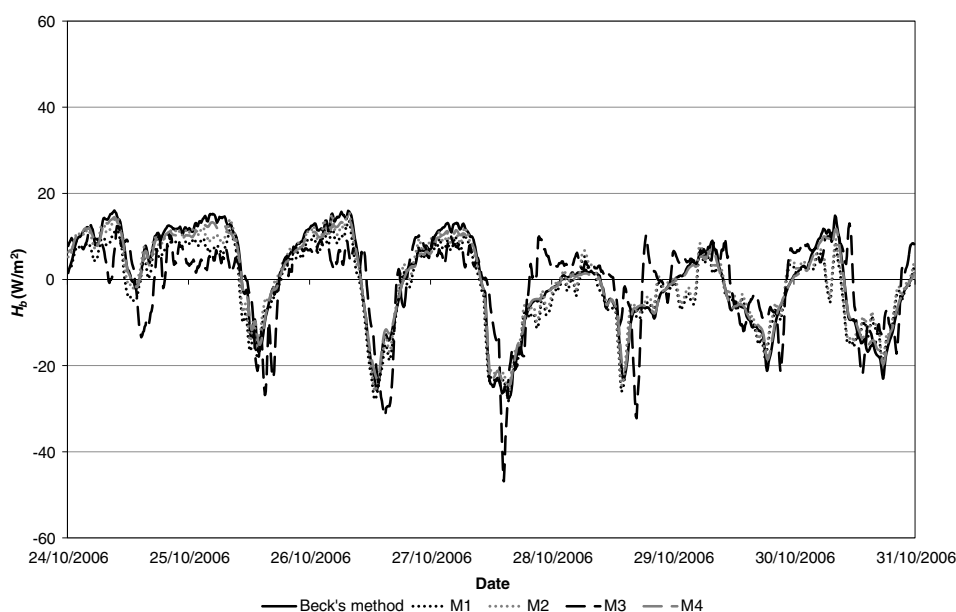


Fig. 14. Sediment-water heat exchange, calculated with Beck's method and estimated with Models M1–M4 from October 25, 2006–October 31, 2006

Model M2 at Lucio del Lobo was second best, and Model M1 at Lucio de Vetallengua was third best.

Fig. 12 shows measured and simulated sediment temperature profiles every 6 h during a full day at Lucio de Vetallengua. The simulated profiles are similar to approximately 0.30–0.40 m, which is the active sediment depth. Below this depth, the behavior of simulated temperature differs among the models; however, given that daily temperature variations are insignificant, the variations do not affect heat flux estimations. We cannot determine the active depth from measured temperatures because of measurement errors, which make deep temperature measurements vary more than estimations, and because of the great distance between sensors.

The detailed 10 min results (Figs. 13 and 14) show that Models M1 and M2 provide similar estimations. Model M4 also follows the measured data quite accurately. Model M3, however, does not provide good estimations when sharp variations exist in H_b (Fig. 13). When the thermal behavior is uniform during the study period, Model M3 results are acceptable (Fig. 14). Fig. 15 compares the 10 min estimations we made using each of the models for the Lucio del Lobo data. We made the calculations separately for each week in the study period. Also in Fig. 15, M3 shows the worst performance, with the highest dispersion and the lowest slope respect to H_b calculated with Beck's SFSM. Errors in estimating sediment-water heat flux may result from the models' differing abilities to

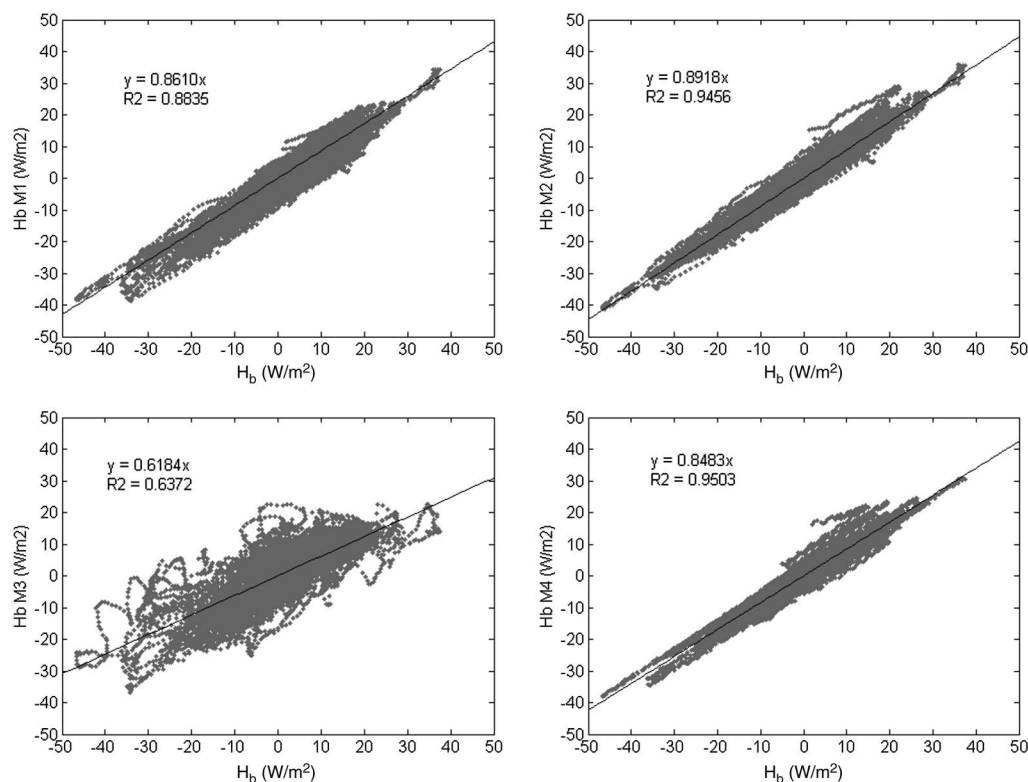


Fig. 15. 10-min simulated heat flux versus measured heat flux, Lucio de Vetalegua (Doñana National Park), October 18, 2006–July 16, 2007

consider the effect of heat flux components for duration longer than 1 week, especially the annual one.

Discussion and Conclusions

Sediment Temperature Measuring Depth

The depth of sediment affected by a given heat pulse depends on the heat flux duration and the thermal properties of the sediment. For the daily timescale, we have shown in this paper (Fig. 12) that daily temperature variations cannot be appreciated below 0.30–0.40 m, in accordance with daily active sediment depths of 0.25 m and 0.30 m obtained by Jobson (1977) and Hondzo and Stefan (1994), respectively. Given certain sediment thermal diffusivity α_b , it is possible to predict the depth of the heat flux active sediment layer through sensitivity analysis (Hondzo and Stefan 1994). For a sinusoidal surface heat flux, Brutsaert (1982) notes that one can obtain a rough estimation of the penetration of the temperature wave from the exponential term in Eqs. (6) and (11); he states that 95% of daily temperature variation is damped at depth $z_d = 3/\eta_d$ for the daily component of the heat flux, and at $z_y = 3/\eta_y$ for the annual component. For the estimated thermal diffusivities, we would have $z_d = 0.28$ m and $z_y = 5.44$ m at Lucio del Lobo, and $z_d = 0.23$ m and $z_y = 4.32$ m at Lucio de Vetalegua. The calculated z_y explains why the depth of integration of Eq. (3) $L = 6$ m in Models M1 and M2 produced results almost identical to $L = 10$ m. Sediment temperature can be considered constant with time below 6 m.

Influence of Initial Condition

The particular characteristics of aquatic ecosystems often make it difficult to install the probes to measure sediment temperature. Consequently, an initial profile of the sediment temperature is often

unavailable. To solve this problem, Jobson (1977) assumed that the initial temperature was constant with depth—the same assumption made in Model M2. If the study period is long enough, from a certain point onward, the effect of the initial conditions actually disappears and estimations improve. For this reason, in methods M1 and M2, calculations began three days before the weekly period for which we would calculate the sediment–water heat exchange. When one compares the results obtained with methods M1 and M2 with those obtained from M4 and Beck’s SFMS, one sees that they are similar. It seems clear, however, that method M1 requires more time for the initial effect to disappear. We may find the cause in the fact that initial sediment temperature estimation in this case is somewhat coarse and the overall difference of estimated and measured temperatures is higher.

Sediment–Water Heat Flux Calculation from Surface Sediment Temperature

A way to solve the problem of absent sediment temperature measurements is by using a model to calculate H_b that does not require an initial condition and only uses the surface sediment or water temperature. In this paper, we propose two methods to this end: M3 and M4. They are based on the theoretical solution of the heat conduction equation for a semi-infinite solid when the surface temperature has a sinusoidal behavior or can be expressed as a Fourier series, respectively. Model M3 is a simplification of Model M4; it assumes that most temperature variation at the surface is sinusoidal with a daily period and that the mean daily heat flux = 0. It has the advantage of allowing computation of sediment–water heat exchange when little water temperature data are available. For example, one can make an approximate computation of H_b estimating $T_{b,d}$ and C_d in Eq. (10) with the average daily temperature and daily temperature range, respectively. When natural sediment approaches such behavior, the model results are reasonably accurate (Fig. 14).

However, when temperature variations exist at longer periods, or when daily heat flux differs significantly from null heat flux, the corresponding components of heat flux are not taken into account by the model, and simulation results are less accurate (Fig. 13). In fact, an important drawback of this method is its inability to detect the influence of the annual component or passing fronts on heat flux.

Instead, Model M4 can simulate heat pulses of durations as long as 1 week, providing very good results that are comparable to those of Model M2, although these results have a lower computational cost (only 0.4 s used by Model M4 compared to 400 s used by Model M2 for the calculation of heat flux during 1 week). Ideally, in precise heat flux calculations, one should use as much harmonics as necessary to fit Eq. (15) to measured surface temperature with the desired precision. However, if surface sediment temperature or water temperature is not available, one can realize a simplified calculation with chosen harmonics. By analyzing Fig. 5, one can deduce that at the weekly timescale, the most influential components are daily ($1d^{-1}$) and half-daily ($2d^{-1}$). We can easily estimate daily amplitudes as one-half of the daily surface temperature range, whereas we can consider half-daily amplitudes constant, with mean values of approximately $0.15\text{--}0.16^{\circ}\text{C}$ at our study sites. Also, several methods estimate mean daily and weekly water temperatures from air temperatures or weather data (Caissie et al. 1998; Mohseni et al. 1998; Erickson and Stefan 2000; Bogan et al. 2003). Other models allow the estimation of maximum daily water temperatures (Caissie et al. 2001) from air temperatures. One can obtain an approximate value of daily amplitude from the difference between maximum and average daily temperatures. Additionally, an annual component might be added to the series of Eq. (15) (Kothandaraman 1971).

Acknowledgments

The authors would like to thank Doñana National Park and the Estación Biológica de Doñana for assisting with installing instrumentation. The authors would also like to acknowledge the work of Quim Rabadà and Daniel Niñerola in maintaining and installing field instrumentation. This study was funded by the Ministerio de Educación y Cultura (complementary action CMT2007-30881-E/TECNO), by the 6th Framework Program of the European Union (contract GOCE-CT-2006-037081), and by the Confederación Hidrográfica del Guadalquivir.

References

Beck, J., Blackwell, B., and Clair, C. R. (1985). *Inverse heat conduction*, Wiley-Interscience, New York.

Beck, J. V., Blackwell, B., and Haji-Sheikh, A. (1996). "Comparison of some inverse heat conduction methods using experimental data." *Int. J. Heat Mass Transfer*, 39(17), 3649–3657.

Beck, J. V., and Woodbury, K. A. (1998). "Inverse problems and parameter estimation: Integration of measurements and analysis." *Meas. Sci. Technol.*, 9, 839–847.

Bladé, E., and Gómez, M. (2006). "Modelación del flujo en lámina libre sobre cauces naturales: Análisis integrado en una y dos dimensiones." Ph.D thesis, Dept. d'Enginyeria Hidràulica, Marítima i Ambiental, Univ. Politècnica de Catalunya, Barcelona, Spain.

Bogan, T., Mohseni, O., and Stefan, H. G. (2003). "Stream temperature-equilibrium temperature relationship." *Water Resour. Res.*, 39(9), 1245.

Braun, S. (2008). *Discover signal processing: An interactive guide for engineers*, Wiley, Chichester, U.K.

Brown, G. W. (1969). "Predicting temperatures of small streams." *Water Resour. Res.*, 5(1), 68–75.

Brutsaert, W. (1982). *Evaporation into the atmosphere: Theory, history and applications*, D. Reidel, Netherlands.

Caissie, D., El-Jabi, N., and St-Hilaire, A. (1998). "Stochastic modelling of water temperatures in a small stream using air to water relations." *Can. J. Civ. Eng.*, 25(2), 250–260.

Caissie, D., El-Jabi, N., and Satish, M. G. (2001). "Modelling of maximum daily water temperatures in a small stream using air temperatures." *J. Hydrol. (Amsterdam)*, 251(1–2), 14–28.

Carslaw, H. S., and Jaeger, J. C. (1959). *Conduction of heat in solids*, Oxford University, New York.

Crooks, S., Schutten, J., Sheern, G. D., Pye, K., and Davy, A. J. (2002). "Drainage and elevation as factors in the restoration of salt marsh in Britain." *Restor. Ecol.*, 10(3), 591–602.

Delay, W. H., and Seaders, J. (1966). "Predicting temperatures in rivers and reservoirs." *J. Sanit. Engrg. Div.*, 92(1), 115–133.

Dolz, J., Bladé, E., and Gili, J. A. (2005). "Modelo numérico de la hidrodinámica de la Marisma." *Doñana, agua y biosfera*, F. GarcíaNovo and C. Marín Cabrera, eds., Confederación Hidrográfica del Guadalquivir, Sevilla, Spain, 140–150.

Edinger, J. E., Duttweiler, D. W., and Geyer, J. C. (1968). "Response of water temperatures to meteorological conditions." *Water Resour. Res.*, 4(5), 1137–1143.

Edinger, J. E., Brady, D. K., and Geyer, J. C. (1974). "Heat exchange and transport in the environment," *Rep. No. 14 (Publication No. EA 74-049-00-3)*, Electric Research Institute, Palo Alto, CA.

Erickson, T. R., and Stefan, H. G. (2000). "Linear air/water temperature correlations for streams during open water periods." *J. Hydrol. Eng.*, 5(3), 317–321.

Evans, E. C., and Petts, G. E. (1997). "Hyporheic temperature patterns within riffles." *Hydrol. Sci. J.*, 42(2), 199–213.

Evans, E. C., McGregor, G. R., and Petts, G. E. (1998). "River energy budgets with special reference to river bed processes." *Hydrol. Processes*, 12(4), 575–595.

Fang, X., and Stefan, H. G. (1996). "Long-term lake water temperature and ice cover simulations/measurements." *Cold Reg. Sci. Technol.*, 24(3), 289–304.

Fang, X., and Stefan, H. G. (1998). "Temperature variability in lake sediments." *Water Resour. Res.*, 34(4), 717–729.

García-Novó, F., and Marín, C., eds. (2005). *Doñana: Agua y Biosfera*, Doñana 2005 Project: Confederación Hidrográfica del Guadalquivir (Guadalquivir Hydrologic Basin Authority), Sevilla, Spain.

Holmes, T. R. H., Owe, M., De Jeu, R. A. M., and Kooi, H. (2008). "Estimating the soil temperature profile from a single depth observation: A simple empirical heatflow solution." *Water Resour. Res.*, 44, W02412.

Hondzo, M., Ellis, C. E., and Stefan, H. G. (1991). "Vertical diffusion in small stratified lake: Data and error analysis." *J. Hydraul. Eng.*, 117(10), 1352–1369.

Hondzo, M., and Stefan, H. G. (1994). "Riverbed heat conduction prediction." *Water Resour. Res.*, 30(5), 1503–1513.

Incropera, F. P., and DeWitt, D. P. (1996). *Fundamentals of heat and mass transfer*, 4th Ed., Wiley, Chichester, U.K.

Ji, C.-C., Tuan, P.-C., and Jang, H.-Y. (1997). "A recursive least-squares algorithm for on-line 1-D inverse heat conduction estimation." *Int. J. Heat Mass Transfer*, 40(9), 2081–2096.

Jobson, H. E. (1977). "Bed conduction computation for thermal models." *J. Hydraul. Div.*, 103(10), 1213–1217.

Kim, K. S., and Chapra, S. C. (1997). "Temperature model for highly transient shallow streams." *J. Hydraul. Eng.*, 123(1), 30–40.

Kothandaraman, V. (1971). "Analysis of water temperature variations in large river." *J. Sanit. Engrg. Div.*, 97(1), 19–31.

Likens, G. E., and Johnson, N. M. (1969). "Measurement and analysis of the annual heat budget for the sediments in two Wisconsin lakes." *Limnol. Oceanogr.*, 14(1), 115–135.

Liu, J. (1996). "A stability analysis on Beck's procedure for inverse heat conduction problems." *J. Comput. Phys.*, 123, 65–73.

Malcolm, I. A., Soulsby, C., and Youngson, A. F. (2002). "Thermal regime in the hyporheic zone of two contrasting salmonid spawning streams: Ecological and hydrological implications." *Fisheries Manag. Ecol.*, 9, 1–10.

- Marti-Cardona, B., Lopez-Martinez, C., Dolz-Ripolles, J., and Bladè-Castellet, E. (2010). "ASAR polarimetric, multi-incidence angle and multitemporal characterization of Doñana wetlands for flood extent monitoring." *Remote Sens. Environ.*, 114, 2802–2815.
- Mohseni, O., Stefan, H. G., and Erickson, T. R. (1998). "A nonlinear regression model for weekly stream temperatures." *Water Resour. Res.*, 34(10), 2685–2692.
- Moreno, J. M., ed. (2005). "Evaluación preliminar de los impactos en España por efecto del cambio climático." Ministerio de Medio Ambiente y Medio Rural y Marino, Madrid, Spain.
- Raphael, J. M. (1962). "Prediction of temperature in rivers and reservoirs." *J. Power Div.*, 88(2), 157–182.
- Reina, M., Espinar, J. L., and Serrano, L. (2006). "Sediment phosphate composition in relation to emergent macrophytes in the Doñana marshes (SW Spain)." *Water Res.*, 40, 1185–1190.
- Ruiz, F., et al. (2004). "Late Holocene evolution of the southwestern Doñana National Park (Guadalquivir estuary, SW Spain): A multivariate approach." *Palaeogeogr. Palaeoclimatol.*, 204, 47–64.
- Shen, H. T., and Chiang, L. A. (1984). "Simulation of growth and decay of river ice cover." *J. Hydraul. Eng.*, 110(7), 958–971.
- Shenefelt, J. R., Luck, R., Taylor, R. P., and Berry, J. T. (2002). "Solution to inverse heat conduction problems employing singular value decomposition and model-reduction." *Int. J. Heat Mass Transfer*, 45, 67–74.
- Shepherd, B. G., Hartman, G. F., and Wilson, W. J. (1986). "Relationships between stream and intragravel temperatures in coastal drainages, and some implications for fisheries workers." *Can. J. Fish. Aquat. Sci.*, 43, 1818–1822.
- Silliman, S. E., Ramirez, J., and McCabe, R. L. (1995). "Quantifying downflow through creek sediments using temperature time series: One-dimensional solution incorporating measured surface temperature." *J. Hydrol. (Amsterdam)*, 167(1–4), 99–119.
- Sinokrot, B. A., and Stefan, H. G. (1993). "Stream temperature dynamics: Measurements and modeling." *Water Resour. Res.*, 29(7), 2299–2312.
- Sinokrot, B. A., and Stefan, H. G. (1994). "Stream water-temperature sensitivity to weather and bed parameters." *J. Hydraul. Eng.*, 120(6), 722–736.
- Siviglia, A., and Toro, E. F. (2009). "WAF method and splitting procedure for simulating hydro- and thermal-peaking waves in open-channel flows." *J. Hydraul. Eng.*, 135(8), 651–662.
- Smith, N. P. (2002). "Observations and simulations of water-sediment heat exchange in a shallow coastal lagoon." *Estuaries*, 25(3), 483–487.
- Taler, J. (1996). "Theory of transient experimental techniques for surface heat transfer." *Int. J. Heat Mass Transfer*, 39(17), 3733–3748.
- Todd, D. K. (1980). *Groundwater hydrology*, Wiley, New York.
- Tsay, T.-K., Ruggaber, G. J., Effler, S. W., and Driscoll, C. T. (1992). "Thermal stratification modeling of lakes with sediment heat flux." *J. Hydraul. Eng.*, 118(3), 407–419.